Check for updates

Preparation and characterization of magnetic graphene nanocomposite containing Cu(proline)$_2$ as catalyst for asymmetric aldol reactions

M. Kooti[1] · **F. Kooshki**[1] · **E. Nasiri**[1]

Abstract

A new catalyst has been prepared via immobilization of Cu(proline)$_2$ complex onto the surface of magnetic graphene. The fabricated nanocatalyst was characterized by Fourier-transform infrared (FT-IR) spectroscopy, powder X-ray diffraction (PXRD) analysis, vibrating-sample magnetometry (VSM), scanning electron microscopy (SEM), energy-dispersive X-ray (EDX) spectroscopy, transmission electron microscopy (TEM), inductively coupled plasma (ICP) techniques, and elemental analysis. Its catalytic performance was investigated in the aldol reaction using a mild and eco-friendly procedure. The synthesized nanocomposite, which contains Cu(II) center as Lewis acid, was found to be an efficient catalyst for asymmetric aldol reactions, affording corresponding aldol products in high yield and excellent enantiomeric excess (> 90 %). The examined catalyst was prepared from low-cost, easily available starting materials and can be readily isolated by magnetic decantation for recycling and reuse in consecutive reactions without significant loss of activity.

Keywords Graphene · Proline · Copper complex · Aldol reactions · Manganese ferrite · Asymmetric reactions

Introduction

The asymmetric aldol reaction is known as one of the most favored synthetic routes for carbon–carbon bond formation in organic chemistry. Therefore, a great deal of effort has been made to develop innovative approaches to improve the performance of this reaction. Recently, organocatalysis has become a powerful and attractive

✉ M. Kooti
  m_kooti@scu.ac.ir

1 Chemistry Department, Shahid Chamran University of Ahvaz, Ahvaz, Iran

🖄 Springer

methodology for production of useful aldol compounds. Proline is an important small chiral amino acid and one of the most well-known organocatalysts. It is also very easily available in pure form with fairly low price. Due to its unique properties, such as conformational rigidity, proline and its various derivatives have been used as catalysts for asymmetric aldol reactions [1–9].

Despite the advantages of proline and its derivatives as homogeneous catalysts, they suffer from some unavoidable problems, mainly difficulties in separation from reaction media and catalyst recovery. Since catalyst recycling and product purity are important in any chemical industry, heterogeneous catalysts are greatly preferred over their homogeneous counterparts. In recent years, use of transition-metal complexes supported on inorganic matrices to design heterogeneous organocatalysts has received remarkable attention. In this regard, proline has been immobilized on various supports, including mesoporous materials, metals, and layered compounds, to improve its efficiency for catalyzing asymmetric aldolization [10–12]. Moreover, application of supported chiral metal complexes for production of specialty and niche chemicals is of great interest [13–15].

Magnetic nanoparticles (MNPs), especially those of mixed metal oxides such as the wide class of ferrites, have been extensively explored in recent years. These MNPs, either in pristine form or modified with some functional groups, are applied in many areas, including biomedicine, biotechnology, environmental remediation, and biosensing as well as catalysis. Magnetic nanoparticles have also been utilized as new catalyst supports, because the magnetic core allows magnetic manipulation of the catalyst by simple application of an external magnetic field [16–23].

Graphene (G), on the other hand, has emerged as a fascinating support for various catalysts due to its high specific surface area and good chemical and thermal stability. Some graphene-based metallic nanocatalysts, such as $CoFe_2O_4$, Mn_3O_4, Au, Pd, FePt, and PtAu, have shown unique catalytic performance in a wide range of heterogeneous organic reactions [24–36]. We report herein the synthesis of a novel heterogeneous nanocatalyst composed of a $Cu(proline)_2$ complex immobilized on a silica-coated graphene/$MnFe_2O_4$(G/MF) composite. The new nanocomposite [G/MF@SiO_2@$Cu(proline)_2$] was found to be an efficient catalyst for asymmetric aldol reaction without use of organic solvents. Furthermore, the catalyst can be easily separated from reaction media with the aid of a permanent magnet and finally recycled. This green nanocatalyst, which is readily prepared from low-cost materials, can be considered to be a promising catalyst for asymmetric aldol reactions.

Experimental

Chemicals

All reagents were of analytical grade and used as received. Products were characterized by comparison of their physical data, such as FT-IR and ^1H nuclear magnetic resonance (NMR) spectra, with those of known samples. NMR spectra were recorded on a Bruker Advance DPX 400 MHz spectrometer using tetramethylsilane (TMS) as internal standard. FT-IR spectra were obtained using a FT BOMEM

MB102 spectrophotometer. Powder X-ray diffraction (PXRD) patterns were taken with a Philips X-ray diffractometer (model PW1840) over the 2θ range from $10°$ to $80°$ using Cu K_α radiation ($\lambda = 1.54056$ Å). Field-emission (FE)SEM images were obtained using a Hitachi Japan S4160 scanning electron microscope. The magnetic properties of the samples were studied by vibrating sample magnetometry (VSM, Meghnatis Daghigh Kavir Company). The copper content of the G/MF@SiO$_2$@ Cu(proline)$_2$ nanocatalyst was determined using an ICP-atomic emission spectroscopy (AES) instrument (HORIBA JobinYvon, Longjumeau Cedex, France). Gas chromatography (GC) experiments were performed with a Shimadzu GC-16A instrument using a 2-m column packed with silicon DC-200 or Carbowax 20M.

Synthesis of G/MF@SiO$_2$@Cu(proline)$_2$

The copper(II) complex Cu(proline)$_2$ was prepared by adding 2.5 mmol copper(II) chloride dihydrate to hot aqueous solvent (20 mL) containing 5 mmol proline and 5 mmol sodium hydrogen carbonate [37]. The mixture was then stirred in a water bath and, after condensation, poured into an ethyl alcohol/acetone mixture (1:1 ratio). The resulting pale-blue precipitate of Cu(proline)$_2$ was filtered, washed with ethyl alcohol and acetone several times, and dried at room temperature for 5 h. The amount of main elements in Cu(proline)$_2$ complex was found as follows: Anal. Calcd. for $C_{10}H_{14}CuN_2O_6$: C, 37.31; N, 8.71; H, 4.39 %. Found: C, 37.06; N, 8.65; H, 4.94 % by elemental analysis. The copper content of the complex as measured by ICP-AES analysis was 19.46 %. Therefore, according to elemental analysis, the Cu:ligand molar ratio in the copper complex was 1:2.

In a separate step, G/MF was synthesized by dispersing 0.3 g presynthesized graphene into 20 mL deionized water with sonication for 30 min. Then, Fe(NO$_3$)$_3$·9H$_2$O (0.4 M, 25 mL) and Mn(NO$_3$)$_2$·6H$_2$O (0.2 M, 25 mL) were added into the graphene suspension with stirring at room temperature for 5 min, and the pH was adjusted to 11–12 using 6 M NaOH solution. After addition of 1.0 g polyvinylpyrrolidone (PVP) as surfactant to this mixture, it was heated at 80 °C for 2 h. The obtained nanocomposite was then collected by applying a permanent magnet, washed with hot water–ethanol mixture, and finely powdered after drying in an oven at 100 °C for 4 h. The G/MF nanocomposite was coated with silica using the Stöber method [38]. These was achieved by adding tetraethylorthosilicate (TEOS) to G/MF in presence of NH$_3$ to obtain a three-component G/MF@Si nanocomposite. In the subsequent step, 0.70 g G/MFe@Si nanocomposite was stirred in 35 mL ethanol at room temperature for 2 h. To this suspension, 0.35 g Cu(proline)$_2$ dispersed in 5 mL water was added, and the whole mixture was stirred at room temperature for 24 h. The resulting solid [G/MF@SiO$_2$@Cu(proline)$_2$] was separated by magnetic decantation, washed with ethanol, and dried in an oven at 80 °C for 5 h. The amount of copper in this nanocomposite was found to be 0.633 mmol g^{-1} as determined by ICP-AES analysis.

Aldol reactions catalyzed by G/MF@SiO$_2$@Cu(proline)$_2$

A mixture of benzaldehyde and cyclohexanone at molar ratio of 1:2 mmol and nano-catalyst (0.1 g) was stirred at 40–60 °C; the progress of the condensation reaction was monitored continuously by thin-layer chromatography (TLC). Ethyl acetate (10 mL) was then added to the reaction mixture, and the nanocatalyst was magnetically separated and washed with ethyl acetate and dried for reuse in a new aldol reaction. The remaining liquid was washed with saturated aqueous sodium chloride solution (5 mL) and water (10 mL). The organic layer, which contains the product of the aldol reaction, was separated and dried over anhydrous Na$_2$SO$_4$, followed by evaporation of the solvent at room temperature. The remaining residue was then recrystallized in ethanol to give pure aldol product with 98 % yield. The yields in this and other similar reactions were measured by GC analysis. Identification of the products for a number of selected reactions between cyclohexanone and benzaldehyde derivatives was also performed by ^{1}H NMR and GC–mass spectrometry (MS) techniques. The spectral data of selected products are given below.

Selected spectroscopic data

2-(Hydroxyl(phenyl)methyl)cyclohexan-1-one (Table 1, entry 1): ^{1}H NMR (250 MHz, DMSO) δ: 1.68–1.73 (4H, m), 1.84–1.90 (1H, m), 2.01–2.08 (1H, m), 2.22–2.77 (2H, m), 2.42–2.49 (1H, m), 2.78–2.89 (1H, d), 4.18 (1H, t), 7.28–7.63 (4H, m), 7.93–7.96 (1H, m). *Anti/syn*: 69/31, ee value for the *anti*-isomer: 96 %.

2-(Hydroxyl(4-nitrophenyl)methyl)cyclohexan-1-one (Table 1, entry 2): ^{1}H NMR (250 MHz, DMSO) δ: 1.53–1. 73 (4H, m), 1.83–1.87 (1H, m), 1.99–2.1 (1H, m), 2.21–2.32 (2H, m), 2.48–2.67 (1H, m), 3.32 (1H, d), 5.21 (1H, s), 7.52–7.61 (2H, m), 8.13–8.21 (2H, d). *Anti/syn*: 95/5, ee value for the *anti*-isomer: 94 %.

2-(Hydroxy(*p*-tolyl)methyl)cyclohexan-1-one (Table 1, entry 3): ^{1}H NMR (250 MHz, DMSO) δ: 1.49–1.79 (5H, m), 1.98–2.05 (1H, m), 2.23 (2H, m), 2.35 (3H, s), 2.48–2.53 (2H, m), 5.20 (1H, s), 7.24–7.27 (2H, d), 7.81–7.84 (2H, d).

2-(Hydroxy(3-chlorophenyl)methyl)cyclohexan-1-one (Table 1, entry 4): ^{1}H NMR (250 MHz, DMSO) δ: 1.71 (4H, m), 1.80–1.89 (1H, m), 2.01–2.08 (1H, m), 2.32–2.50 (3H, m), 3.35 (1H, d), 4.10 (1H, t), 7.28–7.59 (4H, m). *Anti/syn*: 98/2, ee value for the *anti*-isomer: 94 %.

2-(Hydroxy(3-fluorophenyl)methyl)cyclohexan-1-one (Table 1, entry 6): ^{1}H NMR (250 MHz, DMSO) δ: 1.53–1.69 (4H, m), 1.82–1.90 (1H, m), 2.01–2.11 (2H, m), 2.21–2.24 (1H, m), 2.44–2.79 (1H, m), 3.38 (1H, d), 4.20 (t, 1H), 7.26–7.33 (3H, m), 7.42–7.57 (1H, m). *Anti/syn*: 96/4, ee value for the *anti*-isomer: 93 %.

2-(Hydroxy(*p*-dimethylaminophenyl)methyl)cyclohexan-1-one (Table 1, entry 7): ^{1}H NMR (250 MHz, DMSO) δ: 1.74 (4H, m), 1. 90 (1H, m), 2.21–2.26 (3H, m), 2.48–2.49 (1H, m), 2.44–2.79 (1H, m), 3.03 (6H, s), 3.32–3.34 (1H, m), 6.75–6.79 (2H, d), 7.65–7.69 (2H, d), 9.65 (OH).

2-((2-Chlorophenyl)(hydroxy)methyl)cyclohexanone (Table 1, entry 8): *anti/syn*: 95/5, ee value for the *anti*-isomer: 92 %.

2-(Hydroxy(2-hydroxyphenyl)methyl)cyclohexan-1-one (Table 1, entry 9): ^{1}H NMR (250 MHz, CDCL$_3$) δ: 1.20 (2H, m), 1.48–1.66 (4H, m), 1.92–2.10 (2H, m),

Table 1 Aldol reactions using G/MF@SiO$_2$@Cu(proline)$_2$ as nanocatalyst in solvent-free condition
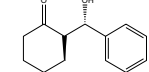
Entry	Aldehyde	ketone	Product[a]	Time (h)	Yield (%)	%ee (anti:syn)
1				5	98	96 69/31
2				5	87	94 95/5
3				5	77	-
4				5	78	94 98/2
5				5	87	-
6				5	87	93 96/4
7				5	82	-
8				5	81	92 95/5
9				5	98	-
10				24	75	-
11				24	70	-
12				24	78	-
13				24	76	-
14				5	95	-
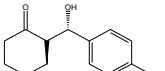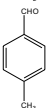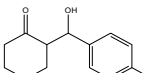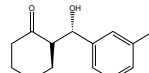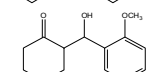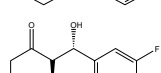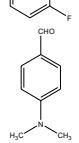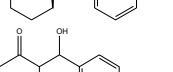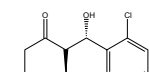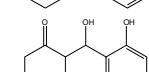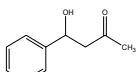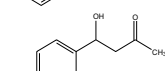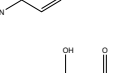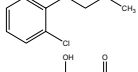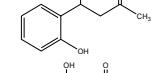
Table 1 (continued)
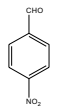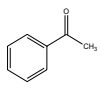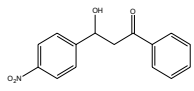
Entry	Aldehyde	ketone	Product[a]	Time (h)	Yield (%)	%ee (anti:syn)
15				5	90	-
16				5	96	-
17				5	85	-
18				5	97	-
19[b]				72	45	95
20				72	43	-
21[c]				72	75	-
22				72	61	-
23				72	30	-
24				72	49	-
25				5	85	-
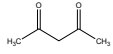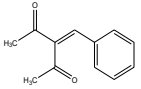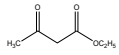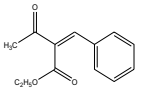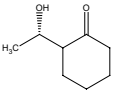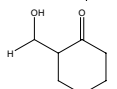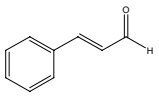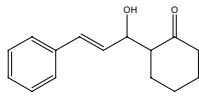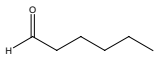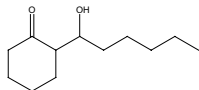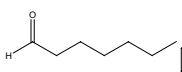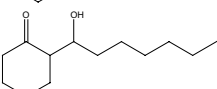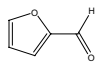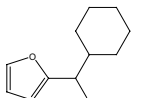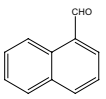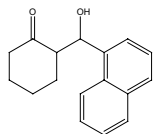
[a]Products were characterized by comparison of NMR, IR, and mass spectroscopy results with reported data

[b]Temperature 20 °C

[c]Temperature 60 °C

2.22–2.25 (1H, m), 2.49 (1H, m), 4.18–4.37 (1H, m), 5.01–5.18 (1H, d), 6.66–6.92 (2H, m), 7.03–7.26 (1H, m), 7.43–7.45 (1H, m).

4-Hydroxy-4-phenylbutan-2-one (Table 1, entry 10), ^{1}H NMR (250 MHz, CDCl$_3$) δ: 2.15–2.19 (1H, br s), 2.38 (3H, s), 2.75–2.97 (2H, d), 5.20 (1H, m), 7.14–7.62 (5H, m).

3-Hydroxy-1,3-diphenylpropan-1-one (Table 1, entry 14), ^{1}H NMR (250 MHz, CDCl$_3$) δ: 2.69 (1H, br s), 3.46 (2H, d), 5.45 (1H, m), 7.30–7.76 (7H, m), 7.89–8.22 (3H, m).

3-Hydroxy-3-(4-nitrophenyl)-1-phenylpropan-1-one (Table 1, entry 15), ^{1}H NMR (250 MHz, CDCl$_3$) δ: 1.34 (1H, CH), 2.69–2.71 (2H, CH$_2$), 7.36–8.39 (9H, m).

3-Hydroxy-3-(2-hydroxyphenyl)-1-phenylpropan-1-one (Table 1, entry 16), ^{1}H NMR (250 MHz, CDCl$_3$) δ: δ: 2.09–2.10 (1H, CH), 2.61 (2H, t), 7.00–7.79 (9H, m).

3-Benzylidenepentane-2,4-dione (Table 1, entry 17): ^{1}H NMR (250 MHz, CDCl$_3$) δ: 2.24–2.38 (7H, 2CH$_3$, CH), 7.35 (5H, m).

Ethyl 2-benzylidene-3-oxobutanoate (Table 1, entry 18): ^{1}H NMR (250 MHz, DMSO) δ: 1.30–1.37 (2H, m), 2.33–2.49 (6H, m), 4.30–4.40 (1H, m), 7.31–7.71 (5H, m).

2-(1-Hydroxyethyl)cyclohexan-1-one (Table 1, entry 19): ee value: 95 %.

Results and discussion

The synthesized nanocatalyst is designated as G/MF@SiO$_2$@Cu(proline)$_2$; its stepwise preparation is shown in Scheme 1. According to the results of various analyses, a structure for the synthesized nanocatalyst is proposed in Scheme 1.

To characterize the as-synthesized nanocatalyst and confirm immobilization of the copper complex on its surface, FT-IR spectroscopy and other techniques were utilized. Figure 1 shows the FT-IR spectra of G/MF (a), Cu(proline)$_2$ (b), and G/MF@SiO$_2$@Cu(proline)$_2$ (c). The FT-IR spectrum of G/MF (Fig. 1a) shows two peaks at 463 cm^{-1} and 582 cm^{-1}, which are assigned to Fe–O stretching at the tetrahedral and octahedral sites of MnFe$_2$O$_4$, respectively. Figure 1b shows the FT-IR spectrum of Cu(proline)$_2$ complex. The peak at 1595 cm^{-1} is related to C=O groups, while the peaks appearing at 1042 and 1116 cm^{-1} are related to stretching of C–O and C–N bonds. In the spectrum for G/MF@SiO$_2$@Cu(proline)$_2$ (Fig. 1c), two peaks at 1092 and 796 cm^{-1} are observed, related to stretching and bending vibration modes of Si–O–Si bonds. The two peaks of MnFe$_2$O$_4$ (471, 587 cm^{-1}) are clearly seen in Fig. 1c for G/MF@SiO$_2$@Cu(proline)$_2$, indicating the presence of this magnetic spinel ferrite in the final composite.

The PXRD patterns of MnFe$_2$O$_4$, Cu(proline)$_2$, and G/MF@SiO$_2$@Cu(proline)$_2$ are presented in Fig. 2. The main peaks at $2\theta = 30.1°$, 36.0°, 43.5°, 57.5°, 57.3°, and 63.1°, corresponding to reflections from (2 2 0), (3 1 1), (4 0 0), (4 2 2), and (3 3 3) planes, respectively, all correspond to MnFe$_2$O$_4$ phase. The same peaks are observed in the PXRD pattern of the G/MF@SiO$_2$@Cu(proline)$_2$ nanocomposite, but with a slight shift to lower 2θ values due to the coating of MnFe$_2$O$_4$ with Cu-proline complex. This observation reveals that MnFe$_2$O$_4$ retained its structure in the synthesized composite.
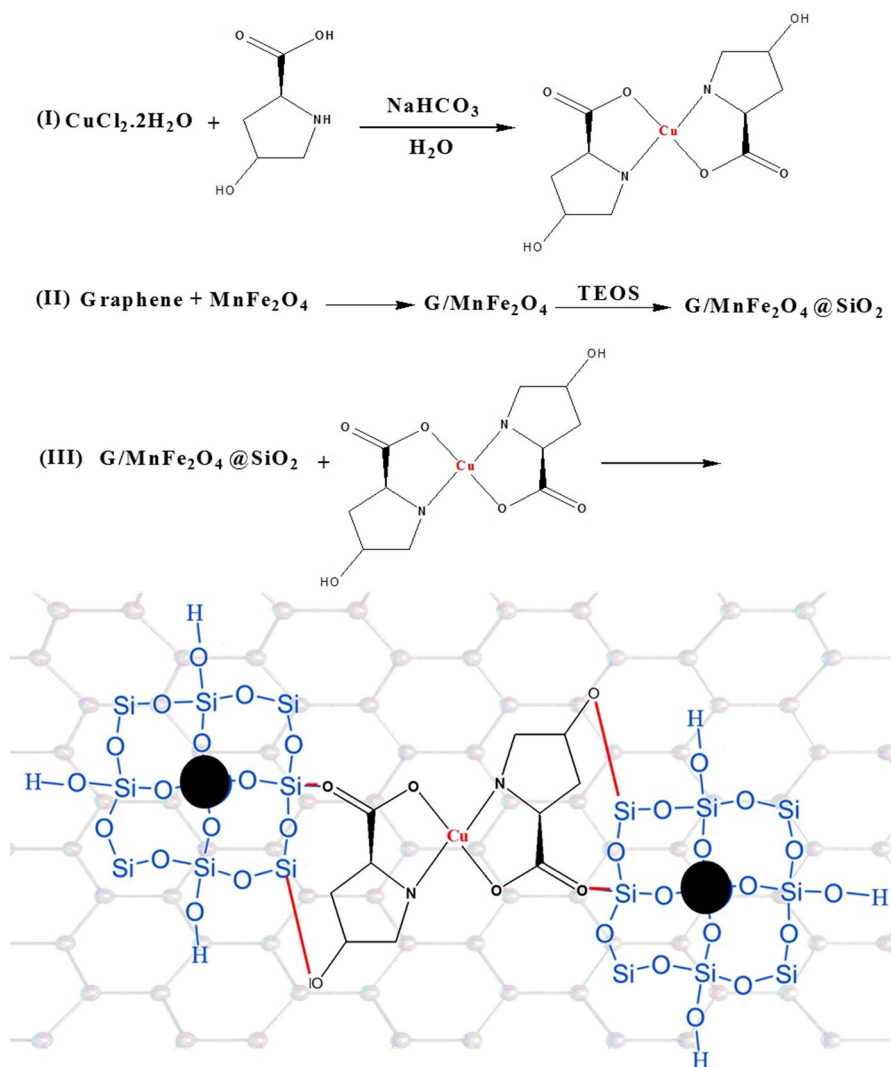
Scheme 1 Stepwise preparation of G/MF@SiO$_2$@Cu(proline)$_2$

A TEM image of the prepared nanocatalyst is depicted in Fig. 3a, clearly showing spherical morphology with slight aggregation. This image indicates that MF@SiO$_2$@Cu(proline)$_2$ (seen as dark spots) is grafted on graphene sheets with particle size distribution of about 25–30 nm. SEM images of all the synthesized samples are also presented in Fig. 3. In these images, graphene shows the expected sheet-like structure (Fig. 3b); after coating with MnFe$_2$O$_4$ only a slight change is observed, and the nanoparticles of this ferrite are well integrated on the surface of graphene (Fig. 3c). The SEM image of G/MF@SiO$_2$@Cu(proline)$_2$ (Fig. 3d) reveals a nearly spherical morphology for this nanocomposite.
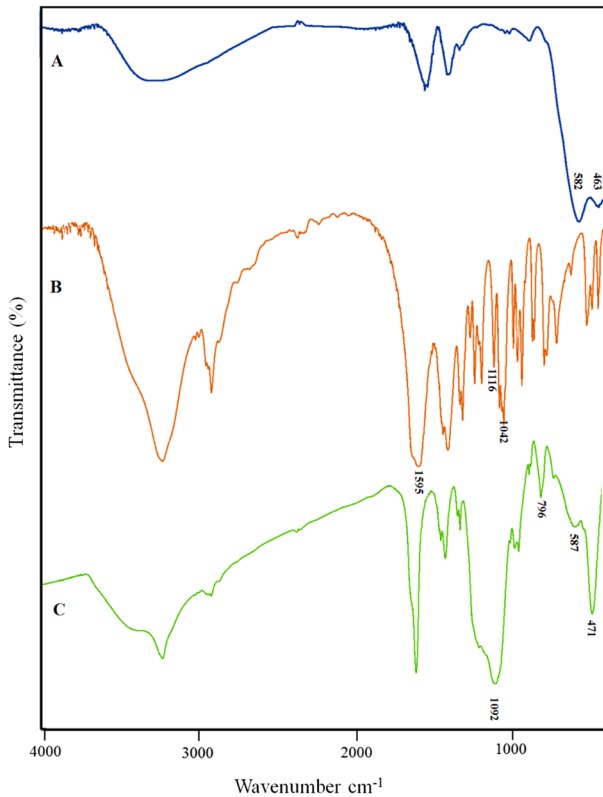
Fig. 1 FT-IR spectra of G/MF (**a**), Cu(proline)$_2$(**b**), and G/MF@SiO$_2$@Cu(proline)$_2$ (**c**)

The composition of the as-fabricated G/MF@SiO$_2$@Cu(proline)$_2$ nanocomposite was further confirmed by EDX analysis. The EDX spectrum of this nanocomposite is shown in Fig. 4, revealing the presence of all main elements, i.e., Mn, Fe, Si, C, N, O, and Cu, composing the nanocomposite.

The magnetic properties of G/MF and G/MF@SiO$_2$@Cu(proline)$_2$ were determined by vibrating sample magnetometry (VSM); the magnetic hysteresis loops are shown in Fig. 5. The VSM curve for the nanocatalyst shows a saturation magnetization (M_s) of only 2 emu g^{-1}, indicating typical superparamagnetic behavior for this composite. The M_s value for this composite is much lower than that of the two-component G/MF composite (6 emu g^{-1}) or pure MnFe$_2$O$_4$. The lower M_s value of this composite may be due to the presence of nonmagnetic silica and Cu(proline)$_2$ complex shells. The magnetization of G/MF@SiO$_2$@Cu(proline)$_2$, however, is still high enough to enable its magnetic separation.

The thermogravimetric analysis (TGA) curve of G/MF@SiO$_2$@Cu(proline)$_2$ catalyst is shown in Fig. 6. The first weight loss (80–180 °C, 1.58 %) corresponds to adsorbed water in the catalyst structure. The seconded weight loss
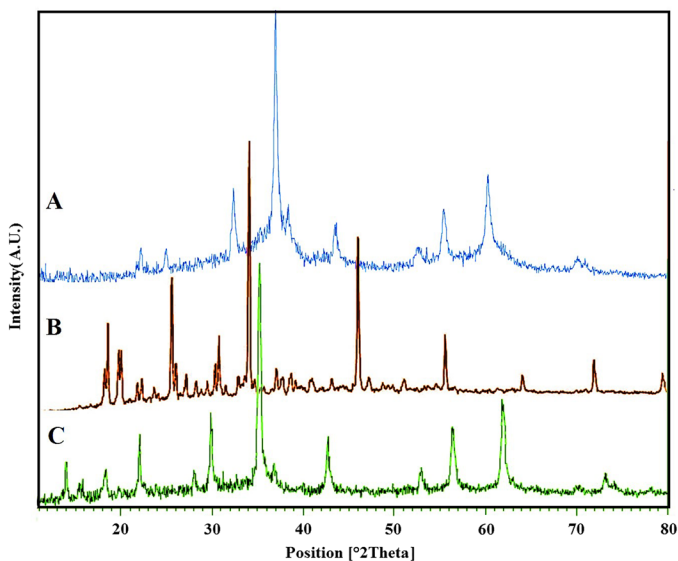
Fig. 2 PXRD patterns of $MnFe_2O_4$ (**a**), $Cu(proline)_2$ (**b**), and $G/MF@SiO_2@Cu(proline)_2$(**c**)

at ~ 190–750 °C is related to release of grafted L-proline of the copper complex and decomposition of the carbon chain of graphene.

We present a green method for one-pot aldol reaction between various aldehydes and some ketones in presence of $G/MF@SiO_2@Cu(proline)_2$ as catalyst. First, aldehydes and ketones were stirred in absence of the catalyst under solventless conditions for 4–5 h. No change in the starting materials was observed according to TLC monitoring of the reaction. However, with addition of nanocatalyst to the reaction mixture, under similar conditions, the reaction proceeded in a period of time to give aldol product in high yield. This result proves that the aldol reaction can only take place in presence of the catalyst. To further explore the scope and limitations of this catalytic system, different aldehydes were tested in the aldol reaction with some ketones under optimized conditions. The results obtained in these reactions are presented in Table 1.

As mentioned above, proline and it derivatives can efficiently catalyze asymmetric aldol reactions. To prove that $G/MF@SiO_2@Cu(proline)_2$ acts as a chiral catalyst, enantiomeric excess (ee) values of some of the products were determined by chiral high-performance liquid chromatography (HPLC) analysis. According to the results, $G/MF@SiO_2@Cu(proline)_2$ showed excellent performance in the direct asymmetric aldol reaction. The ee values of *anti*-isomer, as major enantiomer, for the reaction of cyclohexanone with aromatic aldehydes in free solvent within 5 h was over 90 % (see Figs. S14 to S19).

For further confirmation of the catalytic activity of the designed nanocatalyst, separate experiments for aldol reaction were performed in presence of other samples instead of $G/MF@SiO_2@Cu(proline)_2$. None of the examined materials displayed any catalytic activity for aldol reaction, except proline, $CuCl_2·2H_2O$, and
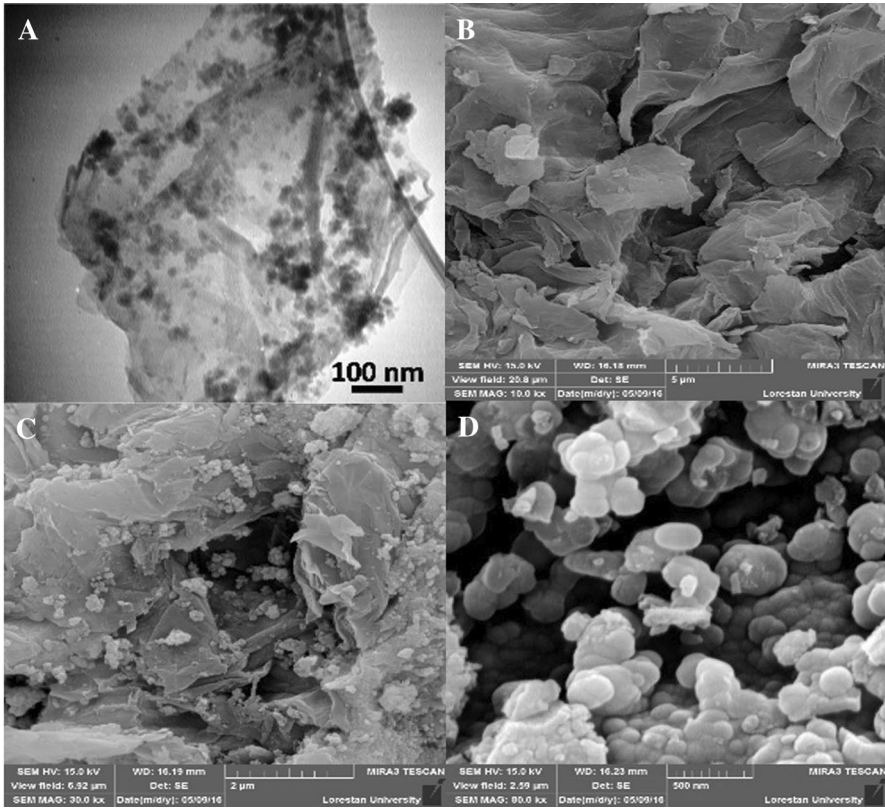
Fig. 3 TEM image of G/MF@SiO$_2$@Cu(proline)$_2$ (**a**) and SEM images of graphene (**b**), G/MF (**c**), and G/MF@SiO$_2$@Cu(proline)$_2$ (**d**)
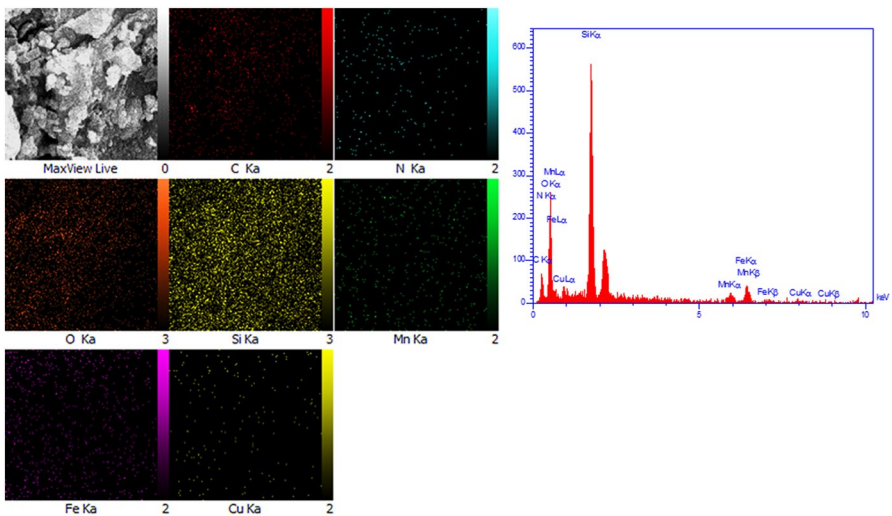
Fig. 4 EDX spectrum of G/MF@SiO$_2$@Cu(proline)$_2$
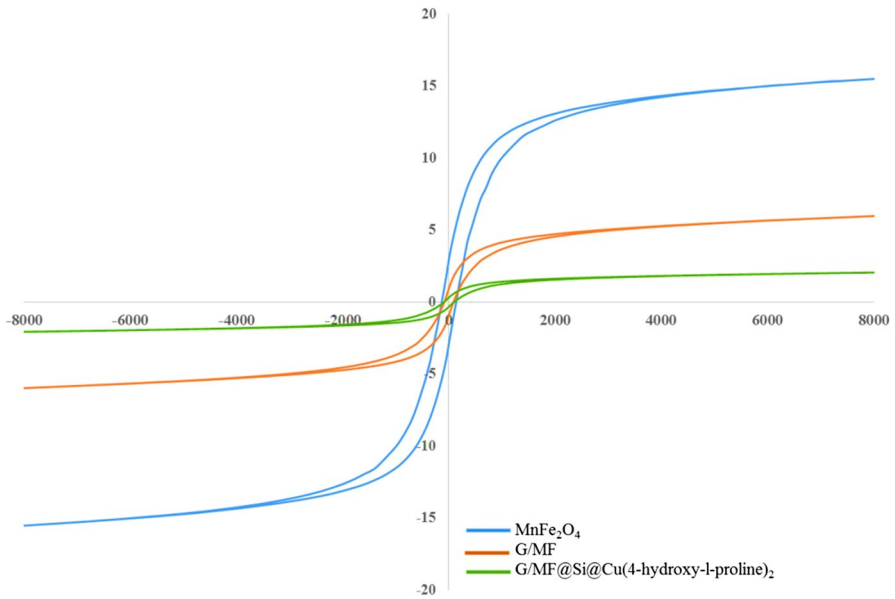
Fig. 5 Hysteresis loops of MnFe$_2$O$_4$, G/MF, and G/MF@SiO$_2$@Cu(proline)$_2$
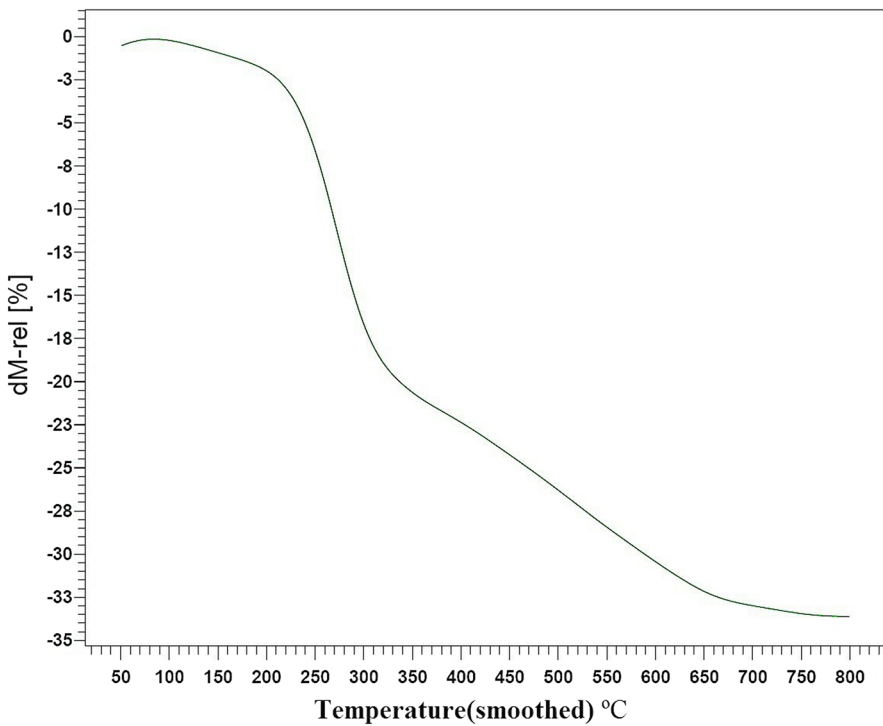
Fig. 6 TGA curve of G/MF@SiO$_2$@Cu(proline)$_2$

Table 2 Comparative study of various materials in aldol reaction

Entry	Nanocatalyst	Yield (%)
1	Graphene	Trace
2	$MnFe_2O_4$	Trace
3	G/MF	Trace
4	G/MF@SiO$_2$	Trace
5	Proline	59
6	$CuCl_2 \cdot 2H_2O$	60
7	Cu(proline)$_2$	65
8	G/MF@SiO$_2$@Cu(proline)$_2$	98

Table 3 Comparison of efficiency of G/MF@SiO$_2$@Cu(proline)$_2$ with other catalysts in aldol reaction

Entry	Catalyst	Solvent	Temperature (°C)	Time (h)	Yield (%)	Ref.
1	Trifluoroacetic acid	H_2O	25	72	46	[39]
2	L-Alanine on graphene	Water	40	24	85	[40]
3	Siloxy-L-serine	Brine	R.t.	12–48	71	[41]
4	2,4-Dinitrobenzenesulfonic acid	Brine	R.t.	12–24	85	[42]
5	Chiral pheboxerhodium	Toluene	60	72	42–75	[43]
6	G/MF@SiO$_2$@Cu(proline)$_2$	Solvent-free	40	5	98	Present

Table 4 Reusability of G/MF@SiO$_2$@Cu(proline)$_2$

Run	Fresh	1	2	3	4	
Yield (%)	98	96	95	93	90	ee: 89 %, *anti/syn*: 73/27

Cu(proline)$_2$, but with lower yield compared with G/MF@SiO$_2$@Cu(proline)$_2$. The results of these experiments are presented in Table 2. This observation indicates that the catalytic activity of the copper complex, Cu(proline)$_2$, was enhanced after it was immobilized on the surface of the G/MFe@SiO$_2$ composite.

To show the advantages of the G/MF@SiO$_2$@Cu(proline)$_2$ catalyst, we compare the results of the present work with other recently reported catalysts used for aldol reactions in Table 3, revealing that the catalyst introduced herein is far superior to the mentioned catalysts in terms of reaction time and conditions.

A facile lifecycle is a major advantage of any heterogeneous catalyst. Therefore, to check the nanocatalyst recovery, the direct aldol reaction of benzaldehyde with cyclohexanone was taken as a model reaction. After reaction completion, the catalyst was separated by applying an external magnetic force and washed with ethyl acetate for three times. After drying the isolated catalyst at 100 °C for 2 h, it was reused in a new aldol reaction with fresh substrates. The catalyst was reused up to five cycles with only negligible loss of activity, as shown in Table 4. Furthermore, the copper content of the recycled nanocatalyst measured by ICP-AES analysis
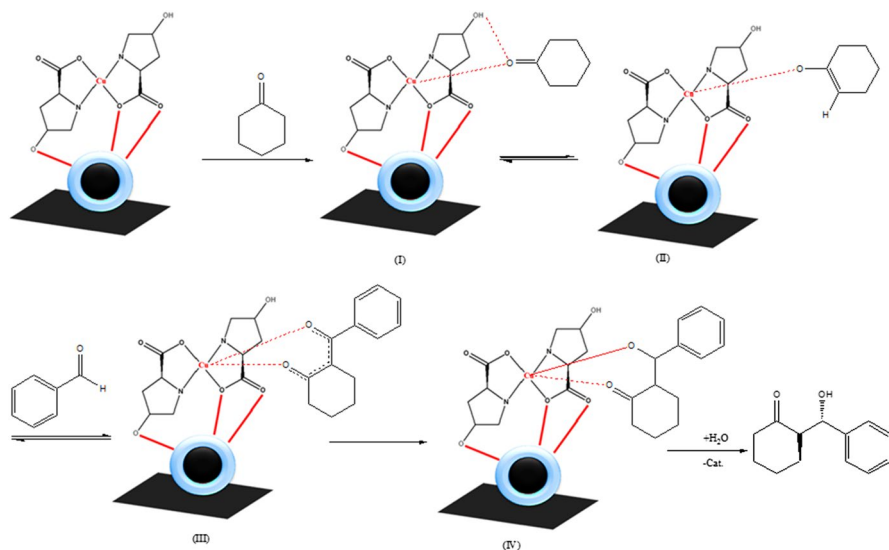
Scheme 2 Proposed mechanism for aldol reaction catalyzed by G/MF@SiO$_2$@Cu(proline)$_2$

after five runs was 0.604 mmol g^{-1}, indicating a loss of only 4.58 % compared with the original catalyst. Therefore, leaching of the catalyst was not great and had no significant effect on its catalytic activity. Also, the ee value for the *anti*-isomer 2-(hydroxyl(phenyl)methyl)cyclohexan-1-one in presence of recycled nanocatalyst after five runs was 89 % (Fig. S20).

According to previous reports in literature [44] and our observations, a mechanism for the aldol reaction is proposed in Scheme 2. First, the carbonyl group of cyclohexanone is activated by metal center of the copper complex in G/MF@ SiO$_2$@Cu(proline)$_2$ nanocatalyst (**I**). This interaction makes the α-hydrogen of the ketone more acidic, which initiates formation of metal–enolate complex **II**. Nucleophilic attack of the carbon–carbon double bond of the enolate moiety on the carbonyl group of benzaldehyde will subsequently occur to produce intermediate **III**. By reorganization of bonding pairs, intermediate **IV** is formed, protonation of which yields the aldol product.

Conclusions

We describe a simple protocol for synthesis of aldol compounds using G/MF@ SiO$_2$@Cu(proline)$_2$ as efficient and magnetically responsive catalyst. Some of the important advantages of this method include mild reaction conditions, high aldol yield, solvent-free conditions, and easy recovery and reusability of the catalyst. The as-prepared catalyst was reused for five times without loss of catalytic

activity. This catalytic procedure performed under solventless conditions with very low leaching of the catalyst can be considered as an environmentally benign approach for aldol reactions.

References

1. M.T. Crimmins, B.W. King, E.A. Tabet, K. Chaudhary, J. Org. Chem. **66**, 894 (2001)
2. L. Li, L.W. Xu, Y.D. Ju, G.Q. Lai, Synth. Commun. **39**, 764 (2009)
3. J. Kofoed, T. Darbre, J.L. Reymond, Chem. Commun. **14**, 1482 (2006)
4. N. Yoshikawa, Y.M.A. Yamada, J. Das, H. Sasai, M. Shibasaki, J. Am. Chem. Soc. **121**, 4168 (1999)
5. V. Sivamurugan, R.S. Kumar, M. Palanichamy, V. Murugesan, J. Heterocyclic Chem. **42**, 969 (2005)
6. B.M. Soares, A.M. Aguilar, E.R. Silva, M.D. Coutinho-Neto, I.W. Hamley, M. Reza, J. Ruokolainene, W.A. Alves, Phys. Chem. Chem. Phys. **19**, 1181 (2017)
7. R. Greco, L. Caciolli, A. Zaghi, O. Pandoli, O. Bortolini, A. Cavazzini, C. De Risi, A. Massi, React. Chem. Eng. **1**, 183 (2016)
8. D.G. Crivoi, R.A. Mirandaa, E. Finocchio, J. Llorca, G. Ramis, J.E. Sueiras, A.M. Segarra, F. Medina, Appl. Catal. A **519**, 116 (2016)
9. Y. Wang, H. Shen, L. Zhou, F. Hu, S. Xie, L. Jiang, Catal. Sci. Technol. **6**, 6739 (2016)
10. Z. An, Y. Guo, L. Zhao, Z. Li, J. He, ACS Catal. **4**, 2566 (2014)
11. S.M. Islam, A.S. Roy, R.C. Dey, S. Paul, J. Mol. Catal. A Chem. **394**, 66 (2014)
12. A. Lu, T.P. Smart, T.H. Epps III, D.A. Longbottom, R.K. O'Reilly, Macromolecules **44**, 7233 (2011)
13. M. Lombardo, F. Pasi, S. Easwar, C. Trombini, Synlett **16**, 2471 (2008)
14. B. List, Tetrahedron **58**, 5573 (2002)
15. D.J. Eyckens, H.L. Brozinski, J.P. Delaney, L. Servinis, S. Naghashian, L.C. Henderson, Catal. Lett. **146**, 212 (2016)
16. S.H. Hosseini, A. Asadnia, J. Nanomater. **2012**, 1 (2012)
17. Y. Jiang, C. Guo, H. Xia, I. Mahmood, C. Liu, H. Liu, J. Mol. Catal. B **58**, 103 (2009)
18. X. Zheng, S. Luo, L. Zhang, J.P. Cheng, Green Chem. **1**, 455 (2009)
19. V. Polshettiwar, R. Luque, A. Fihri, H. Zhu, M. Bouhrara, J.M. Basset, Chem. Rev. **111**, 3036 (2011)
20. J.H. Lee, Y.M. Huh, Y.W. Jun, J.W. Seo, J.T. Jang, H.T. Song, S. Kim, E.J. Cho, H.G. Yoon, J.S. Suh, J. Cheon, Nat. Med. **13**, 95 (2007)
21. R.F. Majidi, N.S. Sanjani, F. Agend, Thin Solid Films **515**, 368 (2006)
22. L.G. Bach, M.R. Islam, J.T. Kim, S.Y. Seo, K.T. Lim, Appl. Surf. Sci. **258**, 2959 (2012)
23. M. Bagheri, M. Masteri-Farahani, M. Ghorbani, J. Magn. Magn. Mater. **327**, 58 (2013)
24. J. Chen, B. Yao, C. Li, G. Shi, Carbon **64**, 225 (2013)
25. S. Sheshmani, R. Amini, Carbohydr. Polym. **95**, 348 (2013)
26. V. Georgakilas, M. Otyepka, A.B. Bourlinos, V. Chandra, N. Kim, K.C. Kemp, P. Hobza, R. Zboril, K.S. Kim, Chem. Rev. **112**, 6156 (2012)
27. D.S. Su, S. Perathoner, G. Centi, Chem. Rev. **113**, 5782 (2013)
28. M.J. Allen, V.C. Tung, R.B. Kaner, Chem. Rev. **110**, 132 (2009)
29. J. Guo, Y. Li, Sh Zhu, Zh Chen, Q. Liu, D. Zhang, W.J. Moon, D.M. Song, RSC Adv. **2**, 1356 (2012)
30. X. Yan, J. Chen, Q. Xue, P. Miele, Micropor. Mesopor. Mater. **135**, 137 (2010)
31. P. Xiong, G. Hu, Y. Fan, W. Zhang, J. Zhu, X. Wang, J. Power Sources **266**, 384 (2014)
32. T. Rakjumar, G.R. Rao, J. Chem. Sci. **120**, 587 (2008)
33. L.T.A. Sofia, A. Krishnan, M. Sankar, N.K. Kala Raj, P. Manikandan, P.R. Rajamohanan, T.G. Ajithkumar, J. Phys. Chem. C **113**, 21114 (2009)
34. Y. Zhang, Y. Zhao, C. Xia, J. Mol. Catal. A **306**, 107 (2009)
35. J. Dupont, R.F. de Souza, P.A.Z. Suarez, Chem. Rev. **102**, 3667 (2002)
36. P. Virtanen, T.O. Salmi, J.P. Mikkola, Top. Catal. **53**, 1096 (2010)
37. Y. Inomata, T. Takeuchi, T. Moriwaki, Inorg. Chim. Acta **68**, 187 (1983)
38. W. Stöber, A. Fink, J. Colloid Interface Sci. **26**, 62 (1968)
39. N. Mase, Y. Nakai, N. Ohara, H. Yoda, K. Takabe, F. Tanaka, C.F. Barbas III, J. Am. Chem. Soc. **128**, 734 (2006)

40. M. Sadiq, R. Aman, K. Saeed, M.S. Ahmad, M.A. Zia, Mod. Res. Catal. **4**, 43 (2015)
41. Y.C. Teo, P.P.F. Lee, Synth. Commun. **39**, 3081 (2009)
42. M. M. Heravi, S. Asadi, Tetrahedron: Asymmetry, **2012**, 23, 1431
43. B.M. Trost, C.S. Brindle, Chem. Soc. Rev. **39**, 1600 (2010)
44. A. Khalafi-Nezhad, E.S. Shahidzadeh, S. Sarikhani, F. Panahi, J. Mol. Catal. A Chem. **379**, 1 (2013)

Publisher's Note Springer Nature remains neutral with regard to jurisdictional claims in published maps and institutional affiliations.